Analysis of heat and mass transfer between air and falling film in a cross flow configuration

A. Ali [a], K. Vafai [b,*], A.-R.A. Khaled [a]

[a] *Department of Mechanical Engineering, Ohio State University (OSU), Columbus, OH 43210, USA*
[b] *Department of Mechanical Engineering, University of California at Riverside (UCR), Bourns Hall, Riverside, CA 92521-0425, USA*

Abstract

Heat and mass transfer between air and falling solution film in a cross flow configuration is investigated. Effects of addition of Cu-ultrafine particles in enhancing heat and mass transfer process are also examined. A parametric study is employed to investigate the effects of pertinent controlling parameters on dehumidification and cooling processes and their subsequent optimization. It is found that low air Reynolds number enhances the dehumidification and cooling processes. An increase in the height and length of the channel and a decrease in the channel width enhance dehumidification and cooling processes. It is also found that an increase in the Cu-volume fraction increases dehumidification and cooling capabilities and produces more stable Cu-solutions.
© 2003 Elsevier Ltd. All rights reserved.

Keywords: Cross flow; Enhancement; Dehumidification

1. Introduction

Desiccant cooling systems have received extensive attention in the past few decades. Liquid desiccant is the salt solution in water and lithium bromide, triethylene glycol, lithium chloride, and calcium chloride are some types of these salt solutions. Liquid desiccants have the ability to absorb moisture from air and then this absorbed moisture can be removed from liquid desiccant by using low grade energy such as waste heat, solar collector, or natural gas. The process of absorbed moisture from the air is called dehumidification and the process of removing this moisture from desiccant is called regeneration. They can be used with the conventional air-conditioning (hybrid air conditioning) to improve the overall performance of the system. They are safe for the environment and result in a reduction in energy consumption and the size of the evaporator and the condenser [1–3].

In this work, the focus will be on the heat and mass transfer between air and solution film, which has a wide range of industrial applications. Elsayed et al. [4] numerically investigated heat and mass transfer between calcium chloride solution and air in counter-flow packed bed arrangement. They obtained the charts needed to predict the outlet conditions of the air and the solution. Park et al. [5] studied coupled heat and mass transfer between air and triethylene glycol solution in a cross flow configuration. They found that a decrease in the mass flow rate of the air resulted in a better control of the humidity ratio and lower temperature for the air. Rahmah et al. [6] analyzed the parallel flow channel between air and solution film in a fin-tube arrangement. They performed a parametric study to investigate the effects of different controlling parameters. Jain et al. [7] investigated liquid desiccant cooling system in a dehumidifier and a regenerator using wetted wall columns. The experimental results agreed with the theoretical model data within 30%. In a recent study, Ali et al. [8] performed a comparative study between air and solution film in parallel and counter-flow configurations with the presence of Cu-ultrafine particles in the solution film.

* Corresponding author. Tel.: +1-909-787-2135; fax: +1-909-787-2899.
E-mail address: vafai@engr.ucr.edu (K. Vafai).

Nomenclature

C_a	humidity ratio of the air ($kg_w\,kg_a^{-1}$)
C_d	concentration of liquid solution ($kg_w\,kg_{sol}^{-1}$)
D	mass diffusivity ($m^2\,s^{-1}$)
d_p	average diameter of ultrafine particles (nm)
g	gravitational acceleration ($m\,s^{-2}$)
H	channel height (m)
k	thermal conductivity ($W\,m^{-1}\,{}^\circ C^{-1}$)
L	channel length (m)
$\dot{m}$	mass flow rate ($kg\,s^{-1}\,m^{-1}$)
N	number of nanoparticles per unit volume
Nu_{AVG}	average Nusselt number
p	total pressure (Pa)
u	velocity in the x-direction ($m\,s^{-1}$)
Re	Reynolds number
T	temperature (°C)
Sh_{AVG}	average Sherwood number
V	volume (m^3)
w	velocity in the z-direction ($m\,s^{-1}$)
W	channel width (m)
x	x-coordinate
y	y-coordinate
z	z-coordinate
Z	salt concentration in the falling film desiccant ($kg_{salt}\,kg_{sol}^{-1}$)

Greek symbols

ρ	density ($kg\,m^{-3}$)
δ	thickness of flow (m)
ϕ	volume fraction (%)
λ	coefficient of thermal dispersion (m)
μ	dynamic viscosity ($N\,s\,m^{-2}$)

Subscripts

a	air
d	desiccant
eff	effective
f	fluid
i	inlet conditions
int	interfacial condition between air and falling film desiccant
m	mean value
o	outlet condition
s	solid
sol	desiccant liquid solution
t	total pressure
ws	saturation pressure
wal	wall
z	vapor pressure of water vapor

Their numerical model was based on a finite difference approximation and a combination of an implicit scheme and iterative method was used to carry out the solution. Their results revealed that the parallel flow arrangement provides better dehumidification and cooling for the air than the counter-flow channel for a wide range of parameters.

Solid metal particles have a much higher thermal conductivity than fluids [9]. As such adding these particles to any working fluid is expected to augment heat and mass transfer within the solid–liquid mixture. Choi [10] studied the enhancement of thermal conductivity of fluids in the presence of nanoparticles and Lee et al. [11] investigated the measurement of thermal conductivity of nanofluids. Xuan and Li [12] used a hot-wire apparatus to measure the thermal conductivity of nanofluids. In a later investigation by Xuan and Roetzel [13], they proposed two different approaches to predict the thermal conductivity of nanosolid–liquid mixture. Both of these approaches will be utilized in this study.

In this work, the heat and mass transfer between air and solution in a cross flow configuration is investigated. Also, ultrafine particles (nanometer) are added to the solution to investigate the enhancements in both heat and mass transfer within the solution. A parametric study is employed to study the effects of pertinent con-

trolling parameters on the dehumidification and cooling processes of the air.

2. Mathematical formulation

The cross flow channel between air and falling solution film is shown in Fig. 1 where the solution film falls vertically over the plate and the air is blown in the z-direction. The assumptions made for this investigations are (1) flow is laminar and steady state, (2) thermal properties of the air and the solution are constant except, for the thermal conductivity of the solution, (3) gravitational force on the air is neglected, (4) thickness of solution is constant, (5) velocity profile is fully developed for both flow regimes, and (6) thermodynamic equilibrium exits at the interface between air and the solution.

2.1. Analysis of cross flow channel between air and solution

The governing mass, momentum, energy, and mass diffusion equations for the air are

$$\frac{\partial w_a}{\partial z} = 0 \tag{1}$$
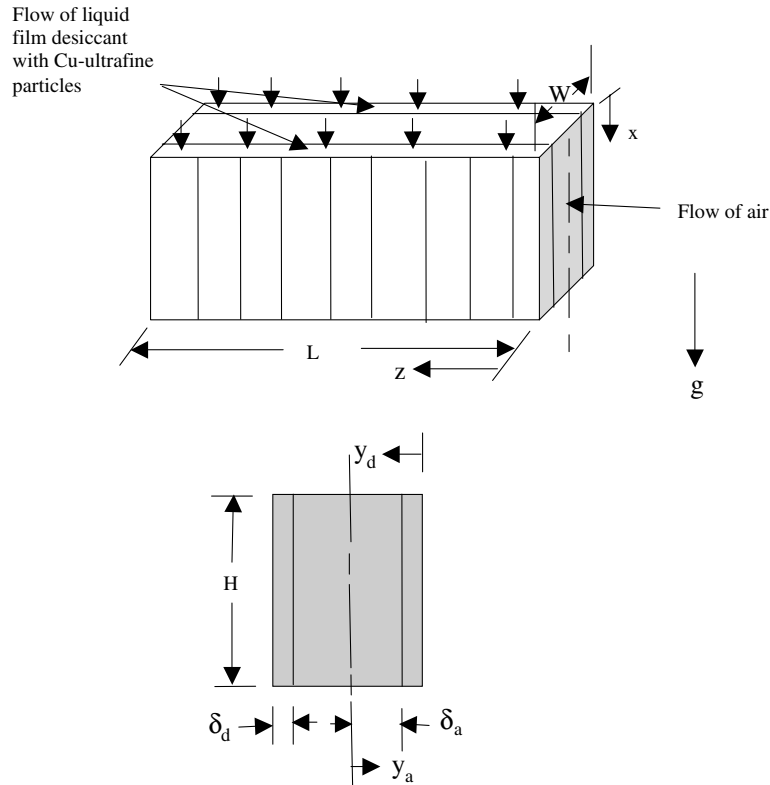
Fig. 1. Schematic of cross flow channel between air and solution.

$$\frac{\partial p_a}{\partial z} = \mu_a \left(\frac{\partial^2 w_a}{\partial y_a^2} \right) \tag{2}$$

$$\rho_a c_{pa} w_a \frac{\partial T_a}{\partial z} = k_a \frac{\partial^2 T_a}{\partial y_a^2} \tag{3}$$

$$w_a \frac{\partial C_a}{\partial z} = D_a \left(\frac{\partial^2 C_a}{\partial y_a^2} \right) \tag{4}$$

The governing mass, momentum, energy and mass diffusion equations for the solution are as follows:

$$\frac{\partial u_d}{\partial x} = 0 \tag{5}$$

$$\rho_d g + \mu_d \left(\frac{\partial^2 u_d}{\partial y_d^2} \right) = 0 \tag{6}$$

$$\rho_d c_{pd} u_d \frac{\partial T_d}{\partial x} = \frac{\partial}{\partial y_d} \left((k_{eff} + k_{dis}) \frac{\partial T_d}{\partial y_d} \right) \tag{7}$$

$$u_d \frac{\partial C_d}{\partial x} = D_d \frac{\partial^2 C_d}{\partial y_d^2} \tag{8}$$

The boundary conditions for the investigation:

$$T_a = T_{ai}, \quad C_a = C_{ai}$$
$$\text{at } z = 0, \ 0 \leqslant x \leqslant H \text{ and } 0 \leqslant y_a \leqslant \delta_a \tag{9}$$

$$T_d = T_{di}, \quad C_d = C_{di}$$
$$\text{at } x = 0, \ 0 \leqslant y_d \leqslant \delta_d \text{ and } 0 \leqslant z \leqslant L \tag{10}$$

$$\frac{\partial w_a}{\partial y_a} = 0, \quad \frac{\partial T_a}{\partial y_a} = 0, \quad \frac{\partial C_a}{\partial y_a} = 0$$
$$\text{at } y_a = 0, \ 0 \leqslant x \leqslant H \text{ and } 0 \leqslant z \leqslant L \tag{11}$$

$$w_a = 0, \quad T_a = T_d, \quad C_a = C_{a_{int}}$$
$$\text{at } y_a = \delta_a, \ 0 \leqslant x \leqslant H \text{ and } 0 \leqslant z \leqslant L \tag{12}$$

where $C_{a_{int}}$ is the interfacial humidity ratio and is given as [14]

$$C_{a_{int}} = 0.62185 \frac{p_z}{(p_t - p_z)} \tag{13}$$

where p_z is equal to [15]

$$p_z = p_{ws} \left(1.0 - 0.828Z - 1.496Z^2 + Z \frac{(T_{int} - 40)}{350} \right) \tag{14}$$

$$u_d = 0, \quad T_d = T_{wal}, \quad \frac{\partial C_d}{\partial y_d} = 0$$
$$\text{at } y_d = 0, \ 0 \leqslant x \leqslant H \text{ and } 0 \leqslant z \leqslant L \tag{15}$$

$$\frac{\partial u_d}{\partial y_d} = 0, \quad T_d = T_a$$
$$\text{at } y_d = \delta_d, \ 0 \leqslant x \leqslant H \text{ and } 0 \leqslant z \leqslant L \tag{16}$$

The energy balance equation at the interface is

$$k_a \frac{\partial T_a}{\partial y_a} + \rho_a D_a h_{fg} \frac{\partial C_a}{\partial y_a} = -k_d \frac{\partial T_d}{\partial y_d}$$

$$\text{at } y_a = \delta_a, \ y_d = \delta_d, \ 0 \leqslant x \leqslant H \text{ and } 0 \leqslant z \leqslant L \quad (17)$$

The mass balance at the interface becomes

$$\rho_a D_a \frac{\partial C_a}{\partial y_a} = -\rho_d D_d \frac{\partial C_d}{\partial y_d}$$

$$\text{at } y_a = \delta_a, \ y_d = \delta_d, \ 0 \leqslant x \leqslant H \text{ and } 0 \leqslant z \leqslant L \quad (18)$$

The velocities for both air and solution are obtained analytically from Eqs. (2) and (6) with the appropriate boundary conditions and they can be cast

$$w_a(y_a) = \frac{1}{2\mu_a} \frac{\partial p}{\partial z} [y_a^2 - \delta_a^2] \quad (19)$$

$$u_d(y_d) = \frac{\rho_d g}{\mu_d} y_d \left[\delta_d - \frac{y_d}{2} \right] \quad (20)$$

where the pressure drop in the air side and the thickness of the solution are equal to

$$\frac{\partial p_a}{\partial z} = -\frac{3\mu_a \dot{m}_a}{2H \rho_a \delta_a^3} \quad (21)$$

$$\delta_d = \left[\frac{3 \dot{m}_d v_d}{\rho_d g} \right]^{1/3} \quad (22)$$

where $\dot{m}_a$ and $\dot{m}_d$ are mass flow rates of air and solution, respectively.

(a)

(b)
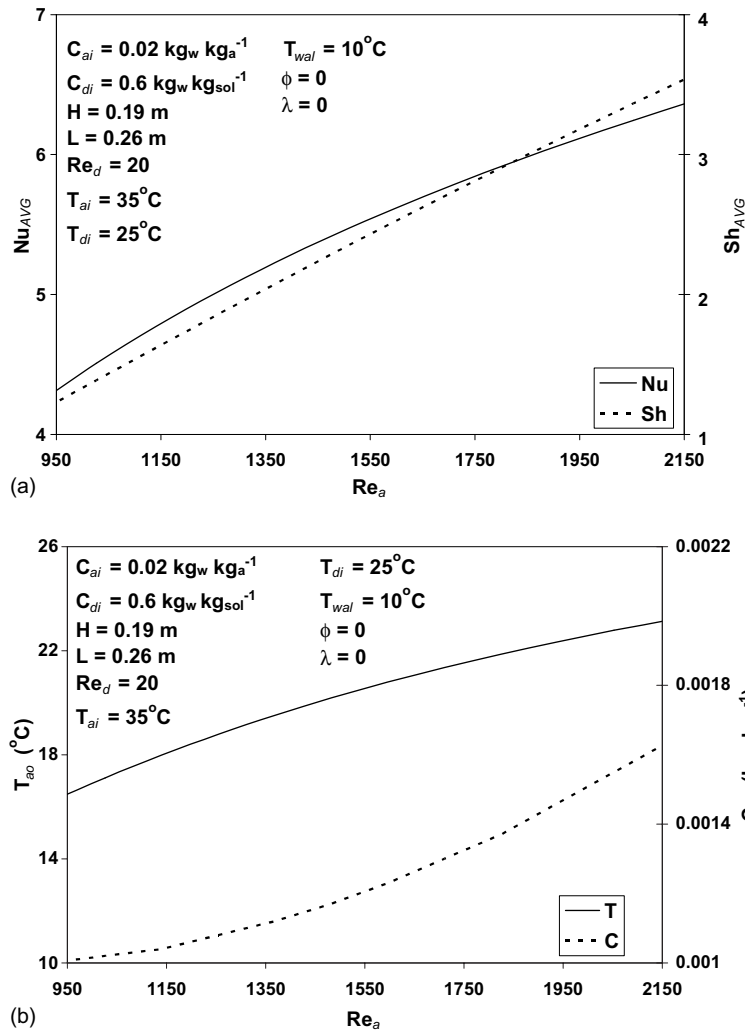
Fig. 2. Effect of air Reynolds number on dehumidification and cooling of the air on (a) Nusselt and Sherwood numbers and (b) exit air conditions.

2.2. Analysis of ultrafine particles in the solution

Two approaches were proposed by Xuan and Roetzel [13] to calculate the thermal conductivity of the nano-fluids. These were the conventional approach and the modified conventional approach where thermal dispersion is taken into account. The modified conventional approach is adopted in this work in which $(\rho C_p)_{eff}$ of the nanofluids can be computed as

$$(\rho C_p)_{eff} = (1 - \phi)(\rho C_p)_f + \phi(\rho C_p)_s \tag{23}$$

where ϕ is the partial volume fraction and defined as [12]

$$\phi = \frac{V_s}{V_f + V_s} = N \frac{\pi}{6} d_s^3 \tag{24}$$

Brinkman [16] extended Einstein's equation for effective fluid viscosity as

$$\mu_{eff} = \mu_f \frac{1}{(1 - \phi)^{2.5}} \tag{25}$$

A relationship was developed by Hamilton and Crosser [17] to calculate the thermal conductivity of solid–liquid mixtures which is valid for thermal conductivity ratio larger than 100:

$$\frac{k_{eff}}{k_f} = \frac{k_s + (n-1)k_f - (n-1)\phi(k_f - k_s)}{k_s + (n-1)k_f + \phi(k_f - k_s)} \tag{26}$$

where k_{eff} in the above equation is considered for conventional single-phase fluid (conventional approach) and n is an empirical factor and defined as

(a)

(b)
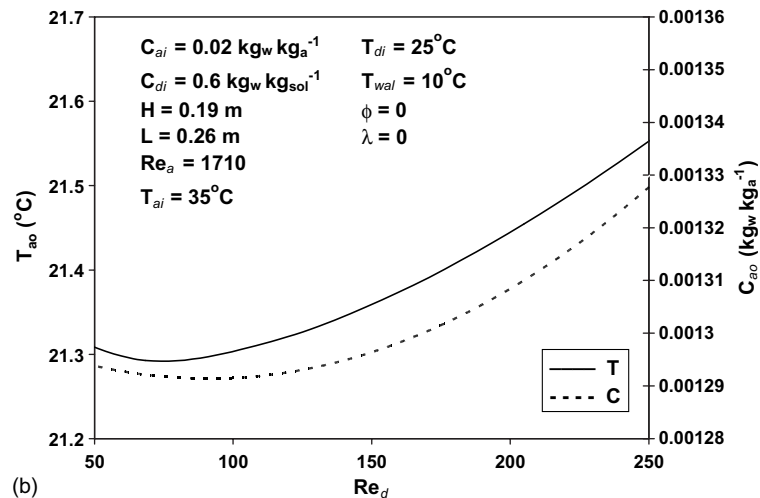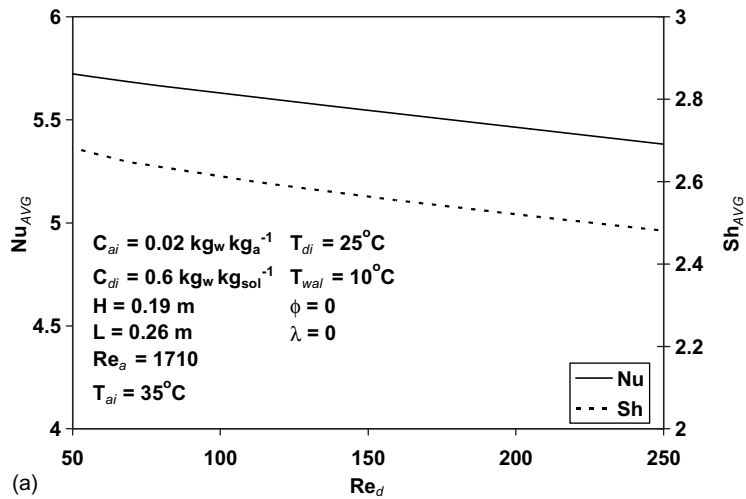
Fig. 3. Effect of solution Reynolds number on dehumidification and cooling of air on (a) average Nusselt and Sherwood numbers and (b) exit air conditions.

$$n = 3/\Psi \tag{27}$$

where Ψ is the sphericity and dispersed thermal conductivity for a porous medium is obtained from [18,19]. The dispersed thermal conductivity of nanofluid can then be written as

$$k_{\mathrm{dis}} = \lambda(\rho C_{\mathrm{p}})_{\mathrm{eff}} u_{\mathrm{d}} \tag{28}$$

where a new constant, λ, is introduced, called coefficient of thermal dispersion, and defined as

$$\lambda = C d_{\mathrm{p}} R \phi \tag{29}$$

where C is a constant, d_{p} is the diameter of the particles, and R is radius of the tube.

In this work, calcium chloride is used as the salt solution and its properties are taken from calcium chloride properties handbook [20]. The moist air properties are obtained from ASHRAE handbook of fundamentals [14] and the properties of Cu-ultrafine particles are acquired from Eastman et al. [21].

2.3. Calculated parameters

The air and solution Reynolds Numbers are defined as

$$Re_{\mathrm{a}} = \frac{4\rho_{\mathrm{a}} w_{\mathrm{am}} \delta_{\mathrm{a}}}{\mu_{\mathrm{a}}} \tag{30}$$

$$Re_{\mathrm{d}} = \frac{4\rho_{\mathrm{d}} u_{\mathrm{dm}} \delta_{\mathrm{d}}}{\mu_{\mathrm{d}}} \tag{31}$$

The average Nusselt and Sherwood Numbers can be cast as follows:
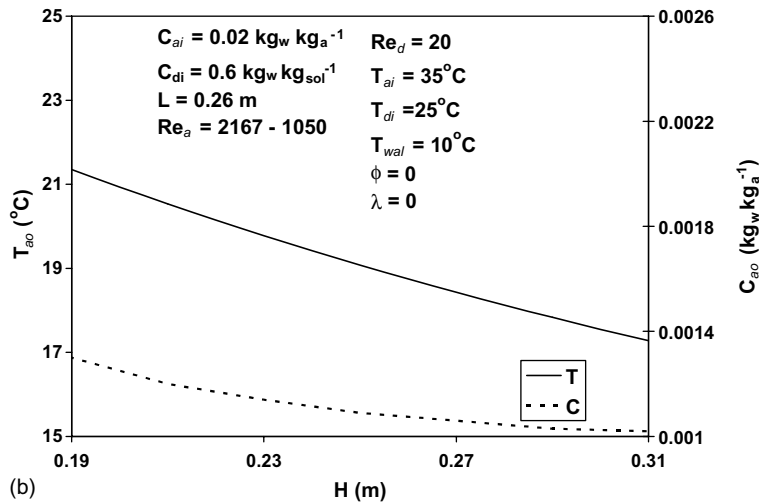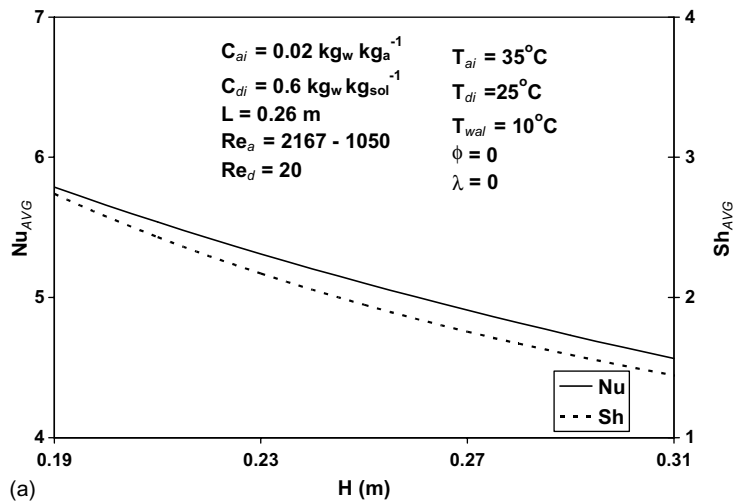
Fig. 4. Effect of channel height on dehumidification and cooling of the air on (a) average Nusselt and Sherwood numbers and (b) exit air conditions.

$$Nu_{\text{AVG}} \equiv \frac{4\delta_a}{LH(T_{ai} - T_w)} \int_0^L \int_0^H \left(\frac{\partial T_a}{\partial y_a} \right)_{y_a = \delta_a} \mathrm{d}x\, \mathrm{d}z \qquad (32)$$

The average Sherwood number can be written as follows:

$$Sh_{\text{AVG}} \equiv \frac{4\delta_a}{LH(W_i - W_{\text{int}})} \int_0^L \int_0^H \left(\frac{\partial W}{\partial y_a} \right)_{y_a = \delta_a} \mathrm{d}x\, \mathrm{d}z \qquad (33)$$

The exit air conditions are calculated based on the mean bulk values Γ_{ao} and can be written as

$$\Gamma_{ao} = \frac{\int_0^H \int_0^{\delta_a} w_j \Gamma\, \mathrm{d}y_a\, \mathrm{d}x}{\int_0^H \int_0^{\delta_a} w_j\, \mathrm{d}y_a\, \mathrm{d}x} \qquad (34)$$

where Γ can be either temperature or humidity ratio.

The effective Peclet number for the film solution which is the ratio of convective to conductive heat transfer is defined as

$$Pe_d = \frac{u_{\text{dm}} \delta_d}{\alpha_{\text{deff}}} \qquad (35)$$

where u_{dm} and α_{deff} are the mean solution velocity and effective thermal diffusivity for the solution, respectively.

3. Numerical analysis

Central finite difference approximations were used for the diffusion terms and the backward difference approximation was used for the axial convection terms. An
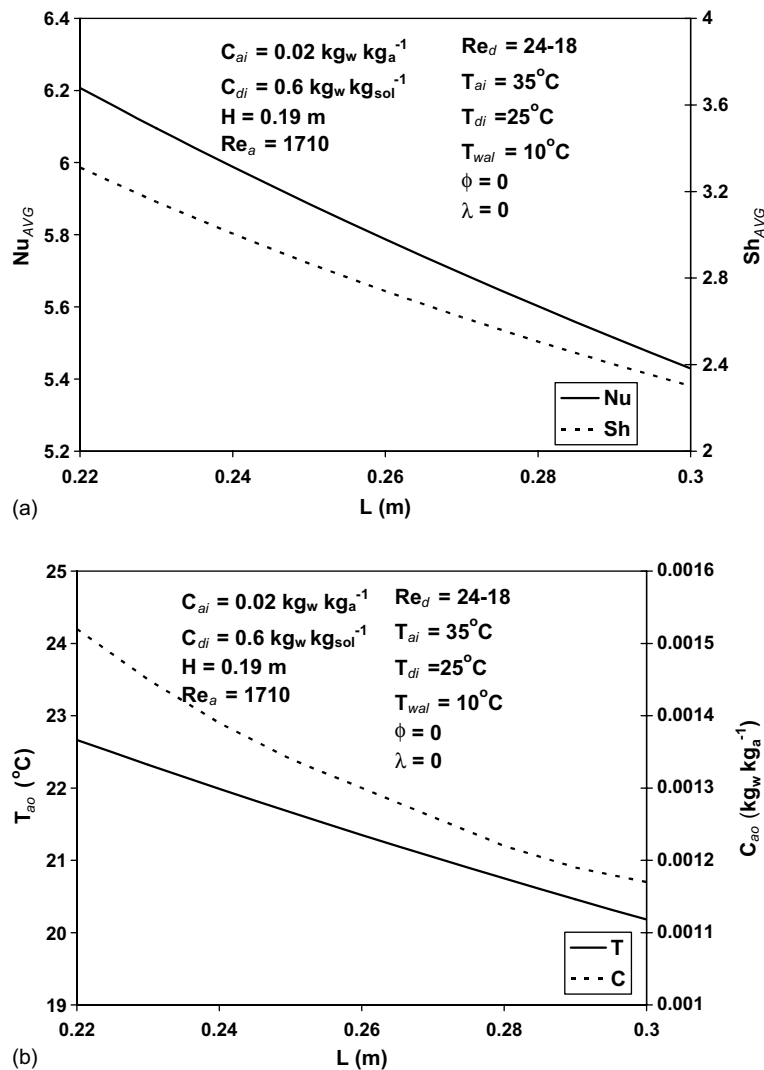
Fig. 5. Effect of channel length on dehumidification and cooling of the air on (a) average Nusselt and Sherwood numbers and (b) exit air conditions.

implicit scheme was utilized to solve the algebraic system of equations using Thomas Algorithm [22]. The form of the discretized equations is as follows:

$$A\Psi_{j-1}^{i+1} + B\Psi_j^{i+1} + AT_{j+1}^{i+1} = F\Psi_j^i \qquad (36)$$

where Ψ could be the temperature, concentration or humidity ratio and A, B, and F are constants depending on fluid properties, dimension of the channel, and grid size. An iterative method is used to satisfy the interfacial conditions between air and solution and the following procedure is employed in the analysis of cross flow configuration:

(a) Input inlet conditions for mass flow rate, temperature, humidity ratio, and concentration for both air and solution and the dimension of the channel.
(b) Calculate the thickness of the solution and then compute the velocity profiles for the solution and air.
(c) Assume interfacial humidity ratio and temperature for the whole domain.
(d) Solve the humidity ratio for the air and concentration for the solution by marching through the whole domain.
(e) Solve the temperature distribution for the solution and air by marching through the whole domain.
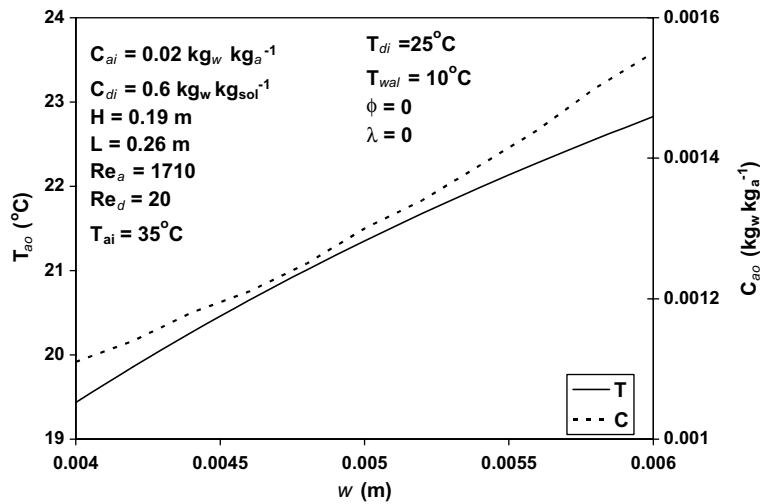
Fig. 6. Effect of channel width on dehumidification and cooling of the air on exit air conditions.
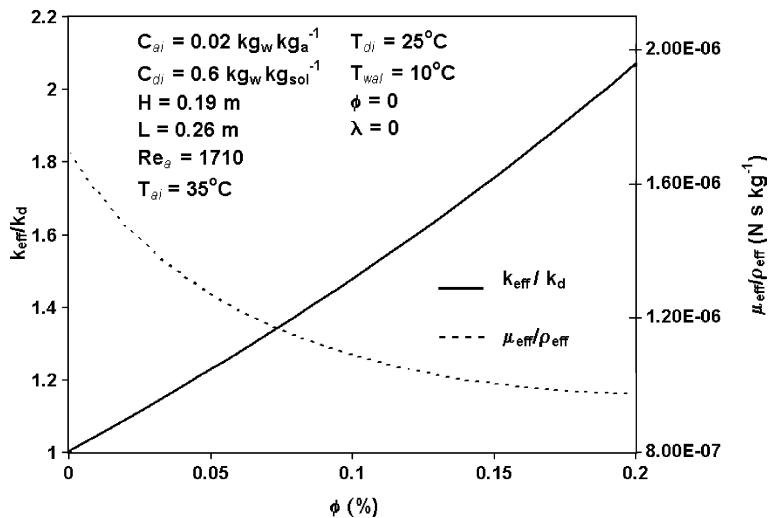
Fig. 7. Effect of volume fraction of Cu-ultrafine particles on ratio of effective thermal conductivity to thermal conductivity of solution and the ratio of effective viscosity to effective density.

(f) Compute the interfacial temperature from equation (17) for the whole domain. If the maximum error between the computed values and assumed one is greater than the convergence criterion, update the assumed values by the computed ones and repeat steps (e)–(f).

(g) If the maximum error between the computed values and assumed one is less than the convergence criterion. Calculate the interfacial humidity ratio from Eq. (13). If the maximum error between the calculated values and assumed ones are greater than the convergence criterion, update the assumed interface values by the calculated values and repeat (d)–(g) until the values of the interfacial humidity ratio converges.

4. Results and discussion

A parametric study is employed to investigate dehumidification and cooling processes of the air in terms of air and solution Reynolds numbers, dimensions of the channel, volume fraction of Cu-ultrafine particles, and thermal dispersion effects. In addition, Cu-ultrafine particles are added to the solution to study the enhancement in heat and mass transfer between the air and the solution.

4.1. Effect of air Reynolds number

Air Reynolds number has a significant effect on the dehumidification and cooling processes of the air. As air
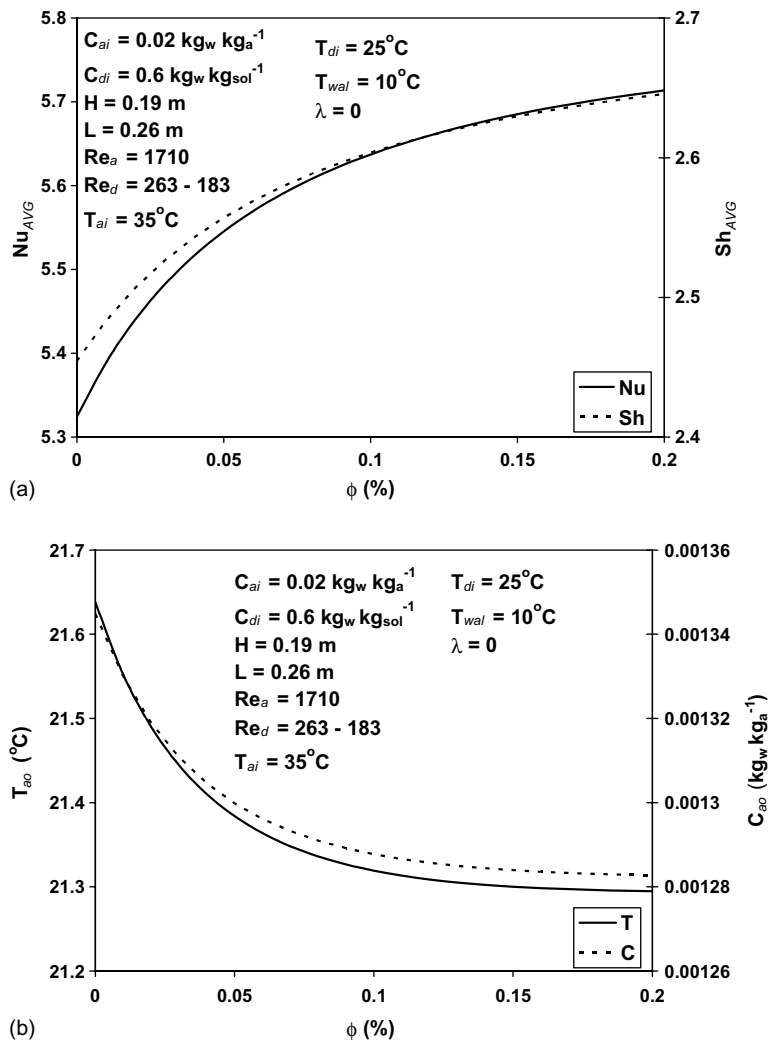
Fig. 8. Effect of volume fraction of Cu-ultrafine particles on dehumidification and cooling of the air on (a) average Nusselt and Sherwood numbers and (b) exit air conditions.

Reynolds number increases, the inlet air conditions convect further out and cause an increase in the temperature and humidity ratio. Therefore, an increase in the air Reynolds number results an increase in both average heat and mass transfer coefficients, which in turn increase the average Nusselt and Sherwood numbers, as illustrated in Fig. 2(a). The air and solution have less time to be in contact with each other at higher air Reynolds numbers which result in higher exit air conditions, as shown in Fig. 2(b). Low air Reynolds number provides better control for exit air conditions.

4.2. Effect of solution Reynolds number

The inlet solution conditions convect further out with an increase in the solution Reynolds number, which results in a decrease in the temperature and humidity difference at the interface. Therefore, the average Nusselt and Sherwood numbers decrease with an increase in solution Reynolds number, as illustrated in Fig. 3(a). There are two important factors in controlling the exit air conditions: (1) enhancement in solution flow due to the increase in flow rate and (2) effect of solution temperature. At low solution Reynolds number, the enhancement in solution flow can be seen. However, this enhancement is diminished due to an increase in solution temperature at High solution Reynolds number. This causes exit air temperature and humidity ratio to decrease slightly at low solution Reynolds number, but increase at high solution Reynolds number, as shown in Fig. 3(b). The increase in the solution Reynolds number reveals a decrease in air passage thickness which enhances the convective transport coefficient; however this effect is not dominant.

4.3. Effect of the channel height

The height of the channel has a substantial impact on the dehumidification and cooling rates of the air. The heat and mass transfer between air and solution decrease further down in the channel, which in turn decrease the temperature and humidity ratio differences at the interface and the average heat and mass transfer coefficients down the channel. Hence, the average Nusselt and Sherwood numbers decrease with an increase in the height of the channel, as illustrated in Fig. 4(a). Fig. 4(b) demonstrates that an increase in the channel height results in significant reduction up to 23% in the exit air temperature and 36% in the exit humidity ratio due to an increase in the residual time and contact surface area between the air and solution at upper values of channel height. These reductions result in better dehumidification and cooling rates for the air which in turn increases the overall efficiency of the air-conditioning system.

4.4. Effect of variations in the length of the channel

The length of the channel has a significant influence on the dehumidification and cooling processes for the air. As seen in Fig. 5(a), the average Nusselt and Sherwood numbers decrease with an increase in the length of the channel due to the same reasoning described with respect to an increase in the height of the channel. Fig. 5(b) reveals reductions up to 11% in the exit air temperature and 22% in the exit humidity ratio with an increase in the length of the channel. These reductions are quite advantageous for the design of air-conditioning systems. It results in a reduction of the overall energy consumption.
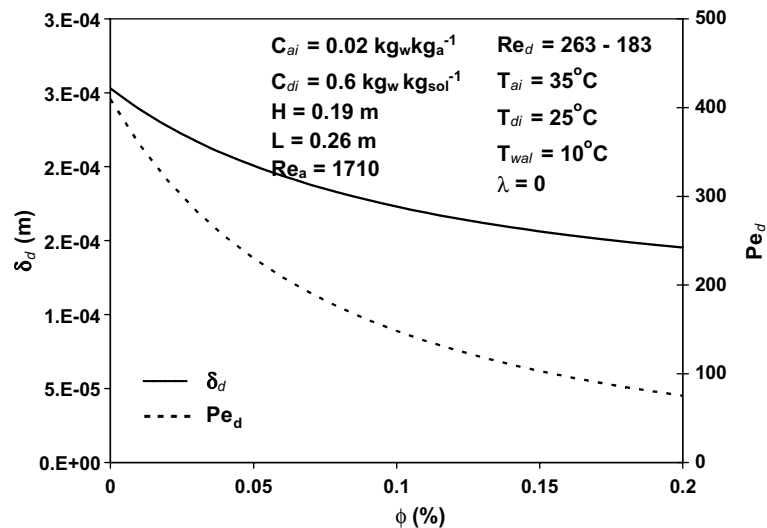
Fig. 9. Effect of partial volume fraction of Cu-ultrafine particles on solution thickness and effective Peclet number.

4.5. Effect of variations in the channel width

Varying the channel width has an impact on the heat and mass transfer between the air and the solution. According to the definitions of both average Nusselt and Sherwood numbers, both values increase as channel width increases. An increase in the width of the channel causes an increase in the air passage thickness while film solution thickness stays unchanged. This increase in the air passage thickness results in a decrease in heat and mass transfer coefficients. This results in an increase in the average air temperature and humidity ratio at the interface resulting in an increase in the exit air conditions, as seen in Fig. 6, therefore poorer dehumidification and cooling rates for the A/C system.

4.6. Effect of the variations in the Cu-ultrafine particles volume fraction

Fig. 7 illustrates the enhancements in the stagnant thermal conductivity with an increase in the Cu-volume fraction as described by Hamilton and Crosser [17] formulation. However, this increase is expected to be more for Cu-ultafine particles in the solution as established in the work of Eastman et al. [9]. This enhancement in the thermal conductivity causes more heat to be transferred from the interface into the solution and therefore from the air. Accordingly, the average Nusselt number increases, as shown in Fig. 8(a). The energy balance at the solution–air interface suggests that an increase in heat transfer to the solution results in an

(a)

(b)
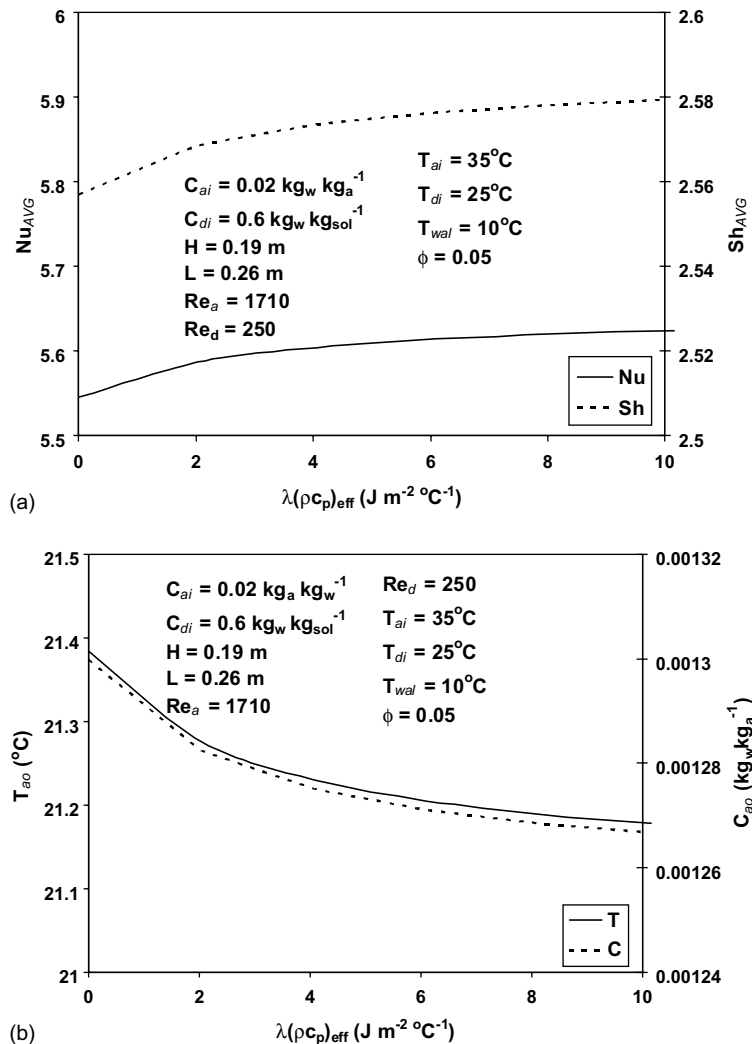
Fig. 10. Effect of dispersion factor of Cu-nanoparticle suspensions for dehumidification and cooling of the air on (a) average Nusselt and Sherwood numbers and (b) exit air conditions.

increase in the rate of water evaporation at the interface thus the average Sherwood number increases as Cu-volume fraction increases. This fact is illustrated in Fig. 8(a). Exit air temperature and humidity are related to the average Nusselt and Sherwood numbers through the integral forms of the energy and mass balances, respectively. These factors reveal that exit air temperature and humidity decrease as Cu-volume fraction increases as illustrated in Fig. 8(b). It is worth noting that noticeable changes in exit air temperature and humidity are expected only at large solution Reynolds numbers since they produce thicker solution films.

4.6.1. Additional mechanisms for heat transfer enhancement

Fig. 9 shows that solution decreases with an increase in the Cu-volume fraction. The presence of ultrafine particles can increase the dynamical stability of the solution due to the associated reduction in the Cu-solution thickness. This reduction minimizes the effects of external disturbances from the air side. Fig. 9 also displays the effect of Cu-volume fraction on the effective Peclet number of Cu-liquid solution. This Peclet number is found to decrease as Cu-volume fraction increases indicating that thermal inlet effects are minimized which in turn maximize the difference between air and solution temperatures.

4.7. Effects of thermal dispersion

Thermal dispersion associated with the random motion of the Cu-ultrafine particels within the solution has a direct impact on enhancing its thermal conductivity. An increase in thermal dispersion increases both average Nusselt and Sherwood numbers, as shown in Fig. 10(a) and decreasing exit temperature and humidity ratio of the air as shown in Fig. 10(b).

5. Conclusions

Enhancement in heat and mass transfer between air and solution in a cross flow channel is investigated in this work. The pertinent controlling parameters are air and solution Reynolds numbers, height, length and width of the channel, and volume fraction and thermal dispersion of the Cu-ultrafine particles. The main conclusions of this investigation are

1. Low air Reynolds number provides better dehumidification and cooling for the exit air conditions.
2. Solution Reynolds number has a minimal effect on dehumidification and cooling processes of the air.
3. An increase in the height and length of the channel offers better dehumidification and cooling for air exit conditions.

4. A decrease in the width of the channel enhances the dehumidification and cooling processes for the exit air conditions.
5. An increase in Cu-volume fraction and thermal dispersion effects enhances the heat and mass transfer and results in a better dehumidification and cooling processes for the air. It also results in dynamically stable solution.

References

[1] J.R. Howel, J.L. Peterson, Preliminary performance evaluation of a hybrid vapor compression/liquid desiccant air conditioning system, ASME, Anaheim, CA, 1986, Paper 86-WA/Sol. 9.

[2] J.W. Studak, J.L. Perterson, A preliminary evaluation of alternative liquid desiccants for a hybrid desiccant air conditioner, in: Proceedings of the Fifth Annual Symposium on Improving Building Energy Effciency in Hot and Humid Climates, Houston, TX, 1988, vols. 13–14, pp. 155–159.

[3] F. Sick, T.K. Bushulte, S.A. Klein, P. Northey, J.A. Duffie, Analysis of the seasonal performance of hybrid desiccant cooling systems, Solar Energy 40 (3) (1988) 211–217.

[4] M.M. Elsayed, H.N. Gari, A.M. Radhwan, Effectiveness of heat and mass transfer in packed beds of liquid desiccant system, Renew. Energy 3 (6–7) (1993) 661–668.

[5] M.S. Park, J.R. Howell, G.C. Vliet, J. Peterson, Numerical and experimental results for coupled heat and mass transfer between a desiccant film and air in cross flow, Int. J. Heat Mass Transfer 37 (Suppl. 1) (1994) 395–402.

[6] A. Rahmah, M.M. Elsayed, N.M. Al-Najem, A numerical investigation for the heat and mass transfer between parallel flow of air and desiccant falling film in a fin-tube arrangement, ASHRAE 6 (4) (2000) 307–323.

[7] S. Jain, P.L. Dhar, S.C. Kaushik, Experimental studies on the dehumidifier and regenerator of a liquid desiccant cooling system, Appl. Therm. Eng. 20 (3) (2000) 253–267.

[8] A. Ali, K. Vafai, A.-R.A. Khaled, Comparative study between parallel and counter flow configurations between air and falling film desiccant in the presence of nanoparticle suspensions, Int. J. Energy Res. 27 (8) (2003) 725–745.

[9] J.A. Eastman, S.U. Choi, W. Yu, L.J. Thompson, Anomalously increased effective thermal conductivities of ethylene glycol-based nanofluids containing copper nanoparticles, Appl. Phys. Lett. 78 (6) (2001) 718–720.

[10] S. Choi, Enhancing thermal conductivity of fluids with nanoparticles, ASME FED 231 (1995) 00–103.

[11] S. Lee, U.S. Choi, S. Li, J.A. Eastman, Measuring thermal conductivity of fluids containing oxide nanoparticles, J. Heat Transfer 121 (2) (1999) 280–289.

[12] Y. Xuan, Q. Li, Heat transfer enhancement of nanofluids, Int. J. Heat Fluid Flow 21 (1) (2000) 58–64.

[13] Y. Xuan, W. Roetzel, Conceptions for heat transfer correlation of nanofluids, Int. J. Heat Mass Transfer 43 (19) (2000) 3701–3707.

[14] ASHRAE Handbook of Fundamentals, SI Ed., American Society of Heating, Refrigeration, and Air-Conditioning, Inc, 1989.

[15] A. Rahmah, Heat and mass transfer between air and a falling film of desiccant solution in a fin-tube arrangement. M.S. Thesis, Kuwait University, Kuwait, 1997.

[16] H.C. Brinkman, Viscosity of concentrated suspensions and solutions, J. Chem. Phys. 20 (1952) 571–581.

[17] R.L. Hamilton, O.K. Crosser, Thermal conductivity of heterogeneous two-component system, I&EC Fundamentals 1 (1962) 182–191.

[18] M.L. Hunt, C.L. Tien, Effect of thermal dispersion on forced convection in fibrous media, Int. J. Heat Mass Transfer 31 (2) (1988) 301–309.

[19] A. Amiri, K. Vafai, Analysis of dispersion effects and non-thermal equilibrium non-Darcian variable porosity incompressible flow through porous medium, Int. J. Heat Mass Transfer 37 (6) (1994) 939–954.

[20] Dow Chemical Company, Calcium chloride properties and forms handbook, Dow Chemical Company, Midland, Michigan, 1983.

[21] J.A. Eastman, U.S. Choi, S. Li, L.J. Thompson, in: S. Komarnenl, J.C. Parker, H.C. Wollenberger (Eds.), Nanocrystalline and Nanocomposite Materials II, vol. 457, Materials Research Society, Pittsburgh, PA, 1997, pp. 3–11.

[22] R.T. Davis, the hypersonic fully-viscous shock-layer problems, Report, SC-RR-68-840, Sanndia Laboratories, 1968.